Published in Heat and Mass Transfer, Vol 37 Iss 4-5 2001

Thermal analysis of an infinite tube during quenching

A. K. Satapathy, R. K. Sahoo

Department of Mechanical Engineering
National Institute of Technology
Rourkela-760008
rksahoo@nitrkl.ac.in

Abstract This paper deals with a numerical solution of the two-dimensional convection–diffusion equation in an infinite domain, arising out of quenching of an infinite tube. On the wetted side, upstream of the quench front, a constant heat transfer coefficient is assumed. The downstream of the quench front as well as the inside surface of the tube are assumed to be adiabatic. The solution gives the quench front temperature as a function of various model parameters such as Peclet number, Biot number and the radius ratio. The solution has been found to be in good agreement with the available analytical solutions and thus validates the numerical procedure suggested.

List of symbols

Bi	Biot number
C	specific heat
h	heat transfer coefficient
k	thermal conductivity
L	length of the tube
Pe	Peclet number
t	time
T	temperature
u	quench front velocity
r, z	physical coordinates
$\bar{r}, \bar{z}$	coordinates in quasi-steady state
R, Z	dimensionless coordinates in quasi-steady state
α	stretching parameter
δ	radius ratio
ρ	density
θ	dimensionless temperature
ξ, η	coordinates after infinite-finite transformation

Subscripts

0	quench front
s	saturation
w	wall condition

1 Introduction

The process of quenching of hot surfaces is of practical importance in nuclear and metallurgical industries. For instance, after a hypothetical loss-of-coolant accident (LOCA) in water cooled reactors, the temperature of the clad surface of the fuel elements would increase drastically because the stored energy in the fuel cannot be removed adequately by the surrounding steam. In order to prevent the fuel from reaching a metallurgically prohibitive temperature, an emergency core cooling system is activated to reflood the core. The time delay in re-establishing effective cooling may result in a cladding temperature rise, significantly above the saturation temperature. If the cladding temperature rises above the rewetting temperature, a stable vapor blanket will prevent the immediate return to liquid–solid contact. Rewetting is the re-establishment of liquid contact with a hot cladding surface and, thereby, bringing it to an acceptable temperature. The quenching phenomenon also exists in numerous industrial applications, such as steam generators, evaporators, cryogenic systems and metallurgical processing.

The cooling process during quenching is characterized by the formation of a wet patch on the hot surface, which eventually develops into a steadily moving quench front. As the quench front progresses along the hot solid, the upstream end of the solid is cooled by convection to the contacting liquid, while its downstream end is cooled by heat transfer to the mixture of vapor and entrained liquid droplets, called precursory cooling. In situations such as low flow rates and top flooding in an open geometry, precursory cooling may be neglected. Besides, from a modeling point of view, even in case of bottom flooding where precursory cooling is important, one may neglect it and compensate it by selecting a higher value of wetside heat transfer coefficient.

The rewetting model for a two-dimensional two-region heat transfer with a step change in heat transfer coefficient at the quench front has been solved for a single slab (Olek 1988), for a composite slab (Olek 1994), for a single rod (Evans 1984) and for composite cylinder (Olek 1989). In the single slab/tube model the unwetted side is considered to be adiabatic, whereas in case of a composite slab/tube a three layer composite is considered to simulate the fuel and the cladding separated by a gas filled gap between them. The rewetting model in a slab geometry with boundary heat flux has been solved by Yao (1977) and Chan and Zhang (1994). The solution methods commonly employed are either separation of variables or Wiener–Hopf technique and the solutions have been obtained for either quench front temperature or quench front velocity.

In the present study, the physical system consists of an infinitely extended vertical tube with outer surface flooded and the inside surface insulated. The model assumes a constant heat transfer coefficient for the wet region whereas the dry region on the flooded side is assumed to be adiabatic. The two-dimensional quasi-steady conduction equation governing conduction-controlled rewetting of the infinite tube has been solved by finite difference method. The numerical model is validated by comparing the results with known closed form solutions. The numerical procedure proposed herewith may be effectively extended to solve the class of rewetting problems that may involve precursory cooling in the dry region or heat flux in the core.

The numerical solution of the rewetting problem encounters two major difficulties: first, the infinite domain of the tube and prescription of the temperature at an infinite boundary. This problem is alleviated by transforming the infinite physical domain to a finite computational domain by a suitable mapping function. The value of the stretching parameter, assigned to the mapping function, has been found by minimizing the overall heat balance. Second, a jump in the boundary condition at the quench front yields a singularity as observed by Blair (1975) and Olek (1988) in the analytical solutions. In the context of the present numerical treatment, the presence of this singularity may give rise to an accuracy problem. This has been overcome by imposing the continuity matching condition for both the temperature and the heat flux at the quench front as described in the text. The numerical solution involves the control volume discretization formulation with power law scheme and then solving the simultaneous algebraic equations by a block iterative method.

2
Mathematical model

The two-dimensional transient heat conduction equation for the tube is

$$\frac{1}{r}\frac{\partial}{\partial r}\left(r\frac{\partial T}{\partial r}\right)+\frac{\partial^2 T}{\partial z^2}=\frac{\rho C}{k}\frac{\partial T}{\partial t},\quad r_1<r<r_2$$

$$\text{and}\ \ 0<z<L,\quad L\to\infty \tag{1}$$

where L is the length of the tube and r_1 and r_2 are inner and outer radius of the tube. The density, specific heat and the thermal conductivity of the slab material are ρ, C and k, respectively. The origin of the coordinate frame is at the bottom point on the axis of the tube. To convert this transient equation into quasi-steady state equation, the following transformation is used:

$$\bar{r}=r\ \ \text{and}\ \ \bar{z}=z-ut$$

where u is the constant quench front velocity and $\bar{r}$ and $\bar{z}$ are radial and axial coordinates, respectively (Fig. 1). Thus the transformed heat conduction equation in a coordinate system moving with the quench front is

$$\frac{1}{\bar{r}}\frac{\partial}{\partial\bar{r}}\left(\bar{r}\frac{\partial T}{\partial\bar{r}}\right)+\frac{\partial^2 T}{\partial\bar{z}^2}+\frac{\rho Cu}{k}\frac{\partial T}{\partial\bar{z}}=0,$$

$$r_1<\bar{r}<r_2,\quad -\infty<\bar{z}<\infty \tag{2}$$

In the conduction controlled rewetting analysis, it is believed that conduction of heat along the solid from dry region to wet region is the dominant mechanism of heat

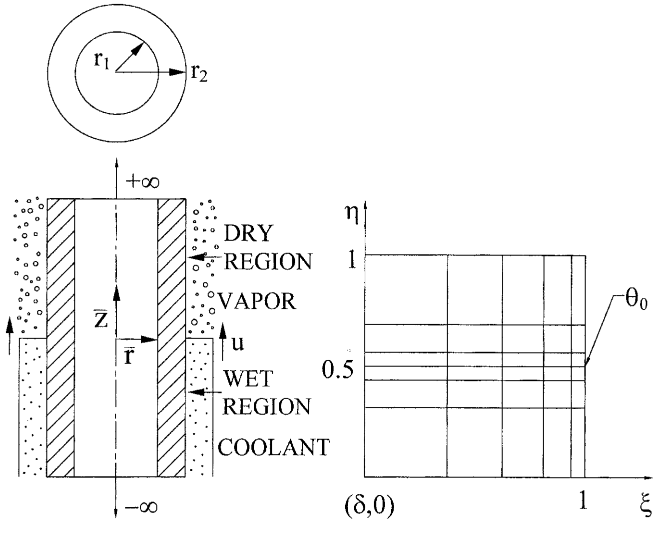

Fig. 1. Physical and computational domain of infinite tube

removal ahead of the quench front, which results in a lowering of the surface temperature immediately downstream of the quench front and causes the quench front to progress further. Since only axial conduction is considered, the effect of coolant mass flux, coolant inlet subcooling and its pressure gradient, etc. are not accounted for explicitly, but only implicitly in terms of wet region heat transfer coefficient, which is incorporated in the boundary condition. In the present analysis, the heat transfer coefficient h is assumed to be constant over the entire wet region. The coolant temperature is taken to be equal to its saturation temperature T_s. Moreover, it is assumed that the far upstream of the quench front (at $\bar{z}\to-\infty$), the wet region is quenched to a temperature T_s, while the far pre-quenched zone (at $\bar{z}\to+\infty$) is still at the initial wall temperature T_w. Equation (2) can be expressed in the following dimensionless form:

$$\frac{1}{R}\frac{\partial}{\partial R}\left(R\frac{\partial\theta}{\partial R}\right)+\frac{\partial^2\theta}{\partial Z^2}+\mathrm{Pe}\frac{\partial\theta}{\partial Z}=0,$$

$$\delta<R<1,\quad -\infty<Z<\infty \tag{3}$$

The associated boundary conditions are:

$$\begin{aligned}
&\frac{\partial\theta}{\partial R}=0\ \ \text{at}\ \ R=\delta,\ \ -\infty<Z<\infty\\
&\frac{\partial\theta}{\partial R}+\mathrm{Bi}\theta=0\ \ \text{at}\ \ R=1,\ \ Z<0\\
&\frac{\partial\theta}{\partial R}=0\ \ \text{at}\ \ R=1,\ \ Z>0\\
&\theta=0\ \ \text{at}\ \ Z\to-\infty\\
&\theta=1\ \ \text{at}\ \ Z\to+\infty
\end{aligned} \tag{4}$$

The non-dimensional variables used above are:

$$R=\frac{\bar{r}}{r_2},\quad Z=\frac{\bar{z}}{r_2},\quad \theta=\frac{T-T_s}{T_w-T_s},$$

$$\mathrm{Bi}=\frac{hr_2}{k},\quad \mathrm{Pe}=\frac{\rho Cur_2}{k},\quad \delta=\frac{r_1}{r_2} \tag{5}$$

Estimation of rewetting (quench front) temperature is essential in predicting the rate at which the coolant quenches the hot surface. The objective of the present study is to compute the temperature field for the given values of Biot number (Bi), Peclet number (Pe) and radius ratio (δ). The non-dimensional quench front temperature is defined by

$$\theta_0 = \frac{T_0 - T_s}{T_w - T_s} \tag{6}$$

where T_0 is the quench front temperature.

The infinite physical domain ($-\infty < Z < +\infty$) is then mapped to a finite computational domain (Fig. 1) by the following infinite–finite transformation:

$$\xi = R \quad \text{and} \quad \eta = 0.5(1 + \tanh \alpha Z) \tag{7}$$

where α is the stretching parameter. The rationale of such a transformation is that the analytical boundary conditions at infinity can be used in the finite-difference equations. The conduction–diffusion equation (3) is thus transformed to

$$\frac{\partial}{\partial \xi}\left(\frac{\xi}{\eta_z}\frac{\partial \theta}{\partial \xi}\right) + \frac{\partial}{\partial \eta}\left(\xi \eta_z \frac{\partial \theta}{\partial \eta} + \xi \mathrm{Pe}\theta\right) = 0,$$
$$\delta < \xi < 1, \quad 0 < \eta < 1 \tag{8}$$

where $\eta_z = \dfrac{\partial \eta}{\partial Z}$.

The transformed boundary conditions are:

$$\begin{aligned}
&\frac{\partial \theta}{\partial \xi} = 0 \ \text{at} \ \xi = \delta, \ 0 < \eta < 1 \\
&\frac{\partial \theta}{\partial \xi} = 0 \ \text{at} \ \xi = 1, \ \eta > 0.5 \\
&\frac{\partial \theta}{\partial \xi} + \mathrm{Bi}\theta = 0 \ \text{at} \ \xi = 1, \ \eta < 0.5 \\
&\theta = 0 \ \text{at} \ \eta = 0 \\
&\theta = 1 \ \text{at} \ \eta = 1 \\
&\theta = \theta_0 \ \text{at} \ \xi = 1, \ \eta = 0.5
\end{aligned} \tag{9}$$

Although Eqs. (8) and (9) have been formulated for quenching by bottom flooding, they are also applicable for top flooding.

3 Numerical solution

The five point representation of the elliptic partial differential equation (8) can be written in the general form

$$A^0_{i,j}\theta_{i,j} = A^1_{i,j}\theta_{i,j+1} + A^2_{i,j}\theta_{i+1,j} + A^3_{i,j}\theta_{i,j-1} + A^4_{i,j}\theta_{i-1,j} \tag{10}$$

The coefficients $A_{i,j}$ are evaluated by applying the power law scheme (Patankar 1980) which makes use of integrating Eq. (8) over non-uniform control volumes, having a face area of $\Delta\xi\Delta\eta$. This approach remains valid for all nodal points except at the quench front. Since discontinuities in boundary conditions exist at the quench front, the coefficients of the discretized equation at this location have been obtained by an appropriate technique (Carnahan et al. 1969). $\theta_{i,j}$ at the interface are expanded into Taylor series ‘forwards’ for the dry region and ‘backwards’ for the wet region, dropping terms beyond second order. These equations give $(\partial^2\theta/\partial\eta^2)_{i,j}$ for the dry and wet regions which, when substituted in non-conservative form of Eq. (8), yields $(\partial\theta/\partial\eta)_{i,j}$ for the dry and wet regions, respectively. Now the expressions for $(\partial\theta/\partial\eta)_{i,j}$ at the interface are put in the following compatibility conditions to determine $A_{i,j}$ of the discretized equation (10):

$$\left(\frac{\partial \theta}{\partial \eta}\right)^{\mathrm{I}}_{i,j} = \left(\frac{\partial \theta}{\partial \eta}\right)^{\mathrm{II}}_{i,j} \quad \text{and} \quad (\theta)^{\mathrm{I}}_{i,j} = (\theta)^{\mathrm{II}}_{i,j}$$

where superscripts I and II denote dry and wet regions, respectively. Expressions for the coefficients in Eq. (10) are tabulated in the Appendix. To solve the system of algebraic equations thus formed, an ADI iterative scheme is used. A convergence criterion of 0.01% change in θ at all nodes has been selected to test the convergence of the iterative scheme. All computations have been carried out using a nonuniform grid arrangement with 21×161 nodes. Since steep temperature gradients are encountered near the quench front, a grid structure has been adopted with finer grids near the quench front and progressively coarser grids away from it (Fig. 1). Sample calculations were also carried out by doubling the grid size to ensure that the results are independent of grid system.

Since the main objective of the present study is to estimate the quench front temperature as correctly as possible, it is essential that the temperature field satisfy the heat balance. This is accomplished by integrating Eq. (8) over the entire computational domain, that gives:

$$\frac{\mathrm{Pe}(1-\delta^2)}{2} = \mathrm{Bi}\int_0^{0.5} \frac{\theta|_{\xi=1}}{2\alpha\eta(1-\eta)}\,\mathrm{d}\eta \tag{11}$$

The integral of Eq. (11) has been obtained using Simpson’s 1/3 rule. Since the integral becomes improper at $\eta = 0$, the indeterminate form at this location has been avoided by applying L’Hospital rule. The absolute difference between the right and left sides of the above equation is first divided by minimum of the two values and then multiplied by 100 to get the percentage difference.

If the heat balance difference so obtained is assumed to be the objective function, then the stretching parameter used in the mapping function can be treated as an independent variable. Thus, starting from an arbitrary base point ($\alpha > 0$), the variable can be moved towards an optimum based on sequential minimization of the objective function. To reduce the number of function evaluations, an optimization technique (Golden Section Search) is used that does not require the derivative of the function. A tolerance limit of 0.01% change of the function value has been selected, below which the search process is terminated.

4 Results and discussion

The numerical computation of the temperature field has been carried out with Bi, Pe and δ as input parameters. In particular, the variation of quench front temperature with respect to the above parameters are shown in the graphical form. First, the distribution of surface temperatures on the coolant side of the slab are plotted (Fig. 2) for different Biot numbers, assuming Pe and δ constant. The quench front temperature is observed to decrease with increase in Biot number. With fixed material properties and dimensions, Biot number represents the heat transfer coefficient. Thus a higher Biot number results in a higher value of the heat transfer coefficient. This enhanced heat transfer coefficient may cause to decrease θ_0. The above trend is in obvious accord with what one would expect on the basis of physical interpretations. θ_0 decreases as Biot number increases, reflecting the fact that a quench front progresses more easily when the heat transfer coefficient to the coolant is increased. Moreover, the temperature gradient also increases with increase in Biot number in Fig. 2. This reveals the fact that at higher values of heat transfer coefficients, the axial conduction across the quench front may be significant.

The dependence of quench front temperature with radius ratio is shown in Fig. 3, for fixed Biot and Peclet numbers. θ_0 is found to increase with decrease in radius ratio δ. With decrease in δ, the thickness of the tube increases and thereby its heat capacity also increases. Thus θ_0 is expected to increase with decrease in δ because of the larger amount of initial heat content in the thicker tube. In the limiting case of a solid rod, where δ is zero, quench front temperature assumes the maximum value.

The variation of quench front temperature with Peclet number is shown in Fig. 4 with $\delta = 0.9$. In this case θ_0 increases with increase in Pe. With fixed material properties and dimensions, Peclet number represents the quench front velocity. For the prescribed radius ratio and Biot numbers, the quench front temperature increases with increase in quench front velocity. This may be due to the fact that a higher relative velocity between the slab and the coolant allows less time for sufficient heat transfer to take place, resulting in a higher value of θ_0. The above trend also reflects the fact that for the same rewetting rate, an increasing cladding thermal diffusivity tends to reduce θ_0.

Finally, the variation of θ_0 with Peclet number is illustrated in Fig. 5 for a solid rod ($\delta = 0$). As expected, the quench front temperature increases with increase in Peclet number and with decrease in Biot number. The present solution has been compared with the analytical solutions of Olek (1989) in Figs. 4 and 5. The agreement is fairly substantial for lower values of Biot numbers, while the accuracy deteriorates when Bi becomes large. This may be due to the mismatch boundary conditions at the quench front. Apparently, the strength of the discontinuity increases with increase in Bi (Eq. (9)) and thus the solution exhibits deviation from the exact results.

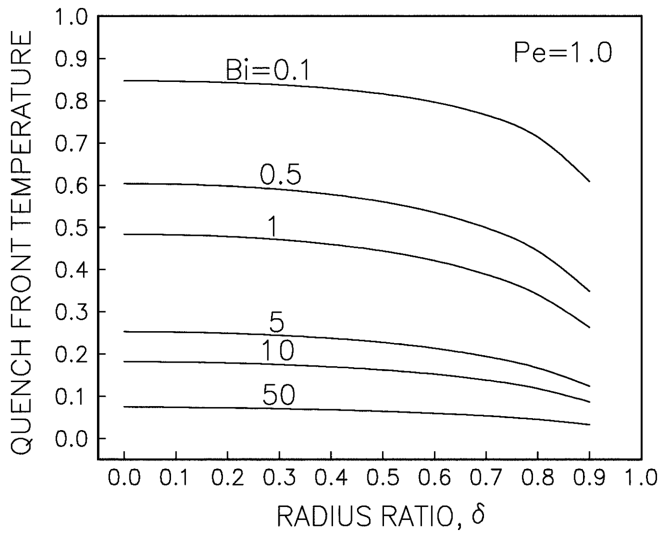

Fig. 3. Quench front temperature variation with radius ratio and Biot number

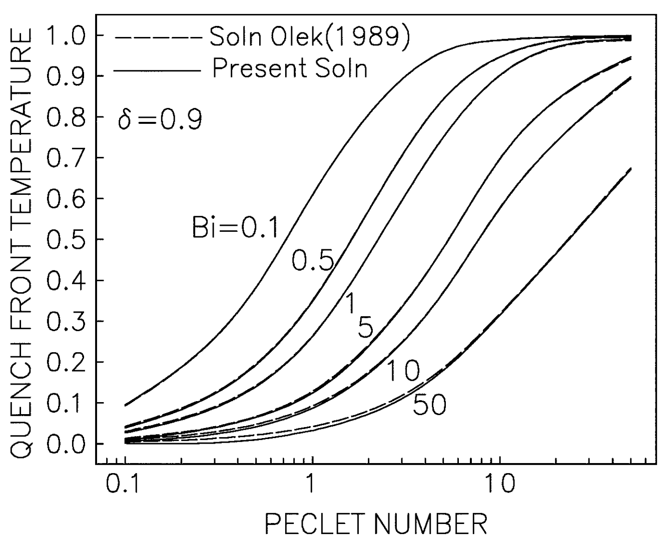

Fig. 4. Quench front temperature variation with Biot and Peclet number for the tube with radius ratio $\delta = 0.9$

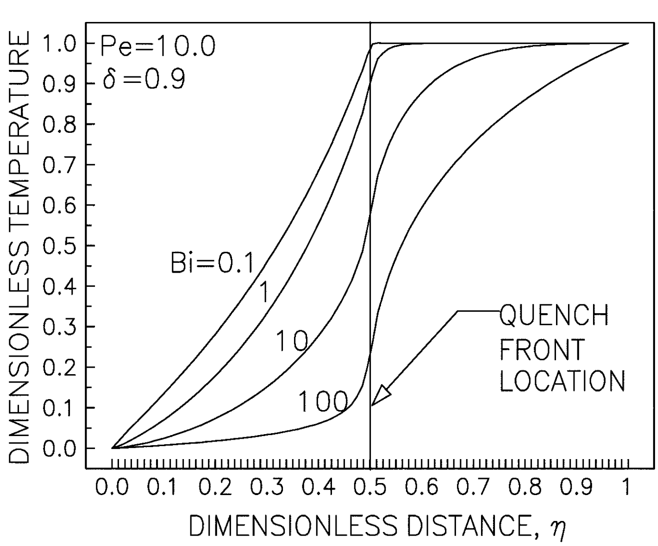

Fig. 2. Surface temperature distribution on the coolant side

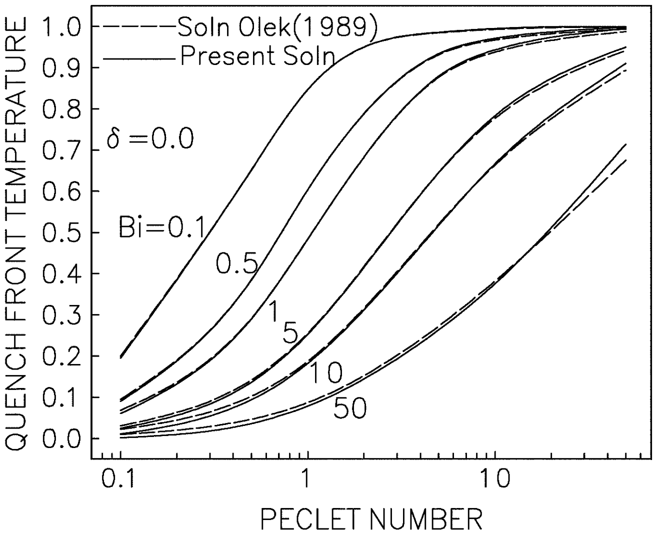

Fig. 5. Quench front temperature variation with Biot and Peclet number for the rod ($\delta = 0$)

5 Conclusion

A numerical solution for solving infinite domain problems arising out of rewetting analysis has been suggested. The value of the stretching parameter used in infinite-finite mapping function can be obtained by minimizing the heat balance. The results computed with non-uniform grids show good agreement with known closed form solutions. In general, quench front temperature is found to increase with increase in Peclet number and with decrease in Biot number. The present solution procedure, in principle, may be extended to other infinite domain rewetting problems involving heat flux in the core or precursory cooling in the dry region.

Appendix: Coefficients of finite difference equations

(a) Internal & boundary nodes (except at the quench front):

$$A^1_{i,j} = f(\xi)\frac{\eta_z^+}{h_2}\left\|0,\left(1-\frac{0.1\mathrm{Pe}h_2}{\eta_z^+}\right)^5\right\| + f(\xi)\cdot\mathrm{Pe},$$

$$A^2_{i,j} = \frac{2f_1 I(\eta)}{h_1}$$

$$A^3_{i,j} = f(\xi)\frac{\eta_z^-}{h_4}\left\|0,\left(1-\frac{0.1\mathrm{Pe}h_4}{\eta_z^-}\right)^5\right\|, \quad A^4_{i,j} = \frac{2f_2 I(\eta)}{h_3}$$

$$A^0_{i,j} = \sum_{k=1}^{4} A^k_{i,j} + 2f_3 I(\eta)$$

For internal nodes:

$$f_1 = \xi^+/(h_1+h_3), \quad f_2 = \xi^-/(h_1+h_3), \quad f_3 = 0,$$
$$f(\xi) = (\xi^+ + \xi^-)/2$$

For boundary nodes:

$$(\xi=\delta) : f_1 = \xi^+/h_1, \quad f_2 = f_3 = 0,$$
$$f(\xi) = (\delta + \xi^+)/2$$
$$(\xi = 1, \eta > 0.5) : f_1 = f_3 = 0, \quad f_2 = \xi^-/h_3,$$
$$f(\xi) = (1+\xi^-)/2$$
$$(\xi = 1, \eta < 0.5) : f_1 = 0, f_2 = \xi^-/h_3, \quad f_3 = \mathrm{Bi}/h_3,$$
$$f(\xi) = (1+\xi^-)/2$$

(b) Quench front node: (ξ = 1, η = 0.5)

$$A^1_{i,j} = \frac{1}{2}\left(\mathrm{Pe}+\frac{\alpha}{h_2}\right)\left(\mathrm{Pe}+\frac{\alpha}{h_4}\right), \quad A^2_{i,j} = 0,$$

$$A^3_{i,j} = \frac{1}{2}\left(\frac{\alpha}{h_4}\right)^2$$

$$A^4_{i,j} = \frac{2}{h_3^2}\left(1+\frac{h_2}{h_4}+\frac{\mathrm{Pe}h_2}{\alpha}\right),$$

$$A^0_{i,j} = \sum_{k=1}^{4} A^k_{i,j} + \mathrm{Bi}\left(1+\frac{2}{h_3}\right)$$

where

$$I(\eta) = \frac{1}{2\alpha}\ln\left[\frac{\eta^+}{\eta^-}\frac{1-\eta^-}{1-\eta^+}\right], \quad \eta_z = 2\alpha\eta(1-\eta),$$
$$h_1 = \xi_{i+1}-\xi_i, \quad h_2 = \eta_{j+1}-\eta_j, \quad h_3 = \xi_i - \xi_{i-1},$$
$$h_4 = \eta_j - \eta_{j-1}$$

Superscripts plus and minus in ξ denote $(i+1/2, j)$ & $(i-1/2, j)$ locations.

Superscripts plus and minus in η denote $(i, j+1/2)$ & $(i, j-1/2)$ locations.

$\| \; \|$ denotes larger between the two values.

References

1. **Blair JB** (1975) An analytical solution to a two-dimensional model of the rewetting of a hot dry rod. Nucl Eng Des 32: 159–170
2. **Carnahan B; Luther HA; Wilkes JO** (1969) Applied Numerical Methods. John Wiley and Sons, NY, p. 462
3. **Chan SH; Zhang W** (1994) Rewetting theory and the dryout heat flux of smooth and grooved plates with a uniform heating. J Heat Transfer (Trans ASME) 116: 173–179
4. **Evans DV** (1984) A note on the cooling of a cylinder entering a fluid. IMA J Appl Math 33: 49–54
5. **Olek S** (1988) On the two-region rewetting model with a step change in the heat transfer coefficient. Nucl Eng Des 108: 315–322
6. **Olek S** (1989) Solution to a fuel-and-cladding rewetting model. Int Commun Heat Mass Transfer 16: 146–158
7. **Olek S** (1994) Quenching of a composite slab. Int Commun Heat Mass Transfer 21: 333–344
8. **Patankar SV** (1980) Numerical Heat Transfer and Fluid Flow. Hemisphere, Washington, p. 96
9. **Yao LS** (1977) Rewetting of a vertical surface with internal heat generation. AIChE Symp Ser 73: 46–50